THE JOURNAL OF PHYSICAL CHEMISTRY A

ARTICLE

pubs.acs.org/JPCA

Computational Evidence for Self-Initiation in Spontaneous High-Temperature Polymerization of Methyl Methacrylate

Sriraj Srinivasan,[†] Myung Won Lee,[‡] Michael C. Grady,[§] Masoud Soroush,[*,†] and Andrew M. Rappe[‡]

[†]Department of Chemical and Biological Engineering, Drexel University, Philadelphia, Pennsylvania 19104, United States

[‡]Makineni Theoretical Laboratories, Department of Chemistry, University of Pennsylvania, Philadelphia, Pennsylvania 19104, United States

[§]Experimental Station, DuPont, Wilimington, Delaware 19898, United States

ABSTRACT: This paper presents computational evidence for the occurrence of diradical mechanism of self-initiation in thermal polymerization of methyl methacrylate. Two self-initiation mechanisms of interest were explored with first-principles density functional theory calculations. Singlet and triplet potential energy surfaces were constructed. The formation of two Diels−Alder adducts, *cis*- and *trans*-dimethyl 1,2-dimethylcyclobutane-1,2-dicarboxylate and dimethyl 2-methyl-5-methylidene-hexanedioate, on the singlet surface was identified. Transition states were calculated using B3LYP/6-31G* and assessed using MP2/6-31G*. The calculated energy barriers and rate constants with different levels of theory were found to show good agreement to corresponding data obtained from laboratory experiments. The presence of a diradical intermediate on the triplet surface was identified. When MCSCF/6-31G* was used, the spin−orbit coupling constant for the singlet to triplet crossover was calculated to be 2.5 cm^{-1}. The mechanism of monoradical generation via a hydrogen abstraction by both triplet and singlet diradicals from a third monomer was identified to be the most likely mechanism of initiation in spontaneous polymerization of methyl methacrylate.

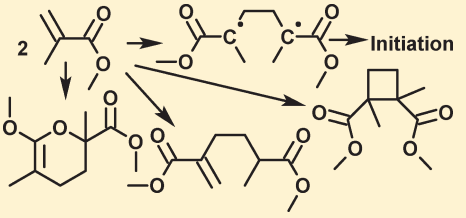

1. INTRODUCTION

There has been significant interest in understanding spontaneous high temperature polymerization of styrene, methacrylates, and more recently alkyl acrylates, because the polymerization can be initiated thermally, in the absence of any known added external initiators.[1−9] Reducing the use of added thermal initiators in thermal free-radical polymerization lowers operating costs and the level of the initiators left unreacted in the end product. The resistance of a coating, an end product, to UV radiation decreases as the level of the unreacted initiators in the coating increases. Understanding the mechanism of the spontaneous initiation is important, as the generated initiating species can be used as controlling agents to produce products with desired properties. Previous studies had speculated that trace quantities of adventitious peroxide impurities, which are difficult to remove from monomers, initiate spontaneous thermal polymerization of methyl methacrylate (MMA).[10,11] However, the absence of end group species from peroxide based impurities and the identification of certain dimer species in solution via gas chromatography−mass spectrometry led to the conclusion that monomer self-initiation may be occurring in spontaneous thermal polymerization of MMA.[1] The two most important self-initiation mechanisms for this class of monomers are the Mayo[2] and Flory[3] mechanisms; the Mayo mechanism is favored for styrene,[5−8] while the Flory mechanism is thought to be responsible in methacrylates and alkyl acrylates.[1,12,13] According to the Mayo mechanism, radical initiating species are formed in two steps. In the first step, the monomers undergo Diels−Alder dimerization, which in the second step (molecular-assisted homolysis) reacts with a third monomer to form monoradicals that initiate the polymerization. In the Flory mechanism, two monomers combine to form a 1,4 singlet (ground state) diradical, which is denoted by $\bullet M\bullet_{2s}$. The 1,4-diradical either reacts with a third monomer and abstracts a hydrogen to form two monoradical initiating species, or undergoes ring closure to form cyclobutane derivatives (Figure 1). Pryor and Lasswell[8] postulated that the 1,4-diradical can initiate polymerization only when it is in a triplet (excited) state. The triplet diradical is denoted by $\bullet M\bullet_{2t}$.

In spontaneous thermal polymerization of MMA, the Diels−Alder adduct (DAA) of MMA was reported to be incapable of generating monoradical species via the molecular assisted homolysis mechanism as in styrene.[1,6] The inability to detect these species in solution[14] provided further evidence that the Mayo mechanism does not generate initiating species in thermal polymerization of MMA. Isolation of cyclobutane derivatives, *cis*- and *trans*-dimethyl 1,2-dimethyl-cyclobutane-1,2-dicarboxylate (DDCD), in solution[15] pointed to the occurrence of a diradical mechanism of self-initiation in spontaneous thermal polymerization of MMA. In addition, high concentrations of the linear dimer, dimethyl 2-methyl-5-methylidene-hexanedioate (DMMH), which is generated via the diradical intermediate route, was reported.[1,14−17] More evidence for the occurrence of the diradical mechanism in self-initiation of MMA came from the

Received: August 14, 2010
Revised: December 1, 2010
Published: January 25, 2011

dx.doi.org/10.1021/jp107704h | *J. Phys. Chem. A* 2011, 115, 1125–1132

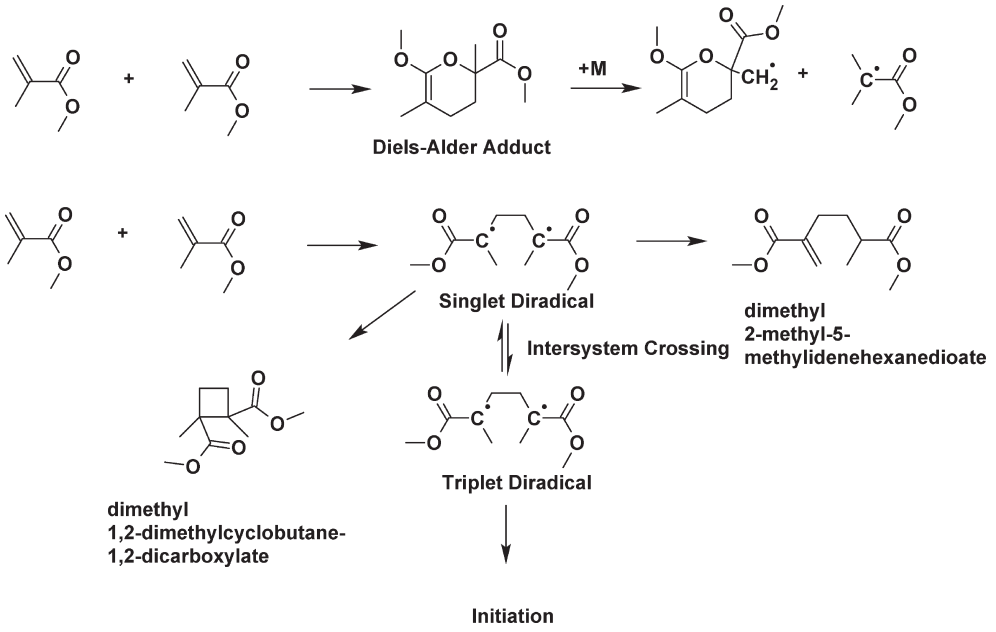

Figure 1. Flory and Mayo mechanisms for self-initiation of methyl methacrylate proposed in previous studies. In this study, our computational results indicate that the singlet diradical can also abstract a hydrogen from a monomer, leading to monoradical generation.

isolation of dimethyl 2,5-dimethylhexanedioate (DDH), which was reported to form via double hydrogen transfer from protic solvents to the 1,4-diradical.[18−20]

Lower conversion (≈5%), higher concentration of dimers, and higher molecular weight polymers were reported in spontaneous polymerization of MMA than in styrene.[8,14−17] The overall rate of spontaneous polymerization of MMA in nonpolar solvents such as benzene was shown to be significantly lower in comparison to that of styrene.[8,21] An increase in the conversion and rate of polymerization was shown to occur in halogenated solvents and thiophenol.[17] It has been postulated[19,22,23] that heavy atoms in halogenated solvents and inert gases can facilitate crossover (intersystem crossing) of the singlet diradical species to a triplet state via collisions. Further evidence of the influence of heavy atoms was provided by the high rate of spontaneous polymerization in chlorinated ethyl methacrylates.[20] The rate of spontaneous thermal initiation in polymerization of MMA was compared and reported to be comparable to the rate of initiation in photochemically initiated polymerization of naphthalene, in which intersystem crossing of diradicals was previously known.[20] On the basis of the similarities, conclusions were drawn that intersystem crossing is probably occurring in the polymerization of MMA. Initiation rate constants estimated using mechanistic models were also used to conclude that the initiating species are the triplet diradicals.[19] One should note that such an analogy is error-prone because the pathways for diradical formation in thermal and photochemical systems have been shown to be different.[24] Furthermore, the estimated initiation rate constants[19] were inconclusive about the true nature of the intermediates that are formed because the model that was used was developed without considering the rate of formation or decomposition of these intermediates. As of yet, there is no evidence to support or deny that (a) the intersystem crossing occurs, (b) the triplet diradicals are formed, or (c) the multiplicity of the diradical species that initiate the polymerization is triplet. In addition, it is unclear if monoradicals can be generated from the triplet diradicals.

High rates of spontaneous high-temperature (>100 °C) polymerization of alkyl acrylates have been reported in the presence of solvents with no heavy atoms.[9,25−28] Also, higher conversion and lower average molecular weight polymers were reported in spontaneous polymerization of alkyl acrylates than in that of MMA.[14,15,26,28] No cyclobutane derivatives or linear dimers in solution have been reported in spontaneous polymerization of acrylates as of yet. It seems that structural differences between acrylate and methacrylate monomers are responsible for the differences in polymer morphology and kinetics of individual reactions.

In general, density functional theory (DFT) has been reported to be a cost-effective and relatively accurate method for predicting molecular geometries and rate constants of polymerization reactions.[12,13,29−32] Previously, DFT calculations using B3LYP/6-31G* have been used to determine the mechanism of initiation in spontaneous thermal polymerization of styrene[32] to be that of Mayo and of methyl, ethyl and n-butyl acrylate[12,13] to be that of Flory. DFT is an exact ground-state technique in principle. However, due to limitations in the current exchange-correlation functionals, DFT chemical reaction transition state energies are not always highly accurate.[33] Calculated transition states can be verified and refined with ab initio methods [Møller−Plesset (MP), Multi-Configuration Self Consistent Field (MCSCF)],[34] and higher level composite methods, such as Gaussian−n (n = 1, 2, 3, 4).[35−39] These methods have been reported to reduce the difference between calculated and experimental values of energy barriers and rate constants. Calculations using these methods for many-atom systems such as MMA, however, can be generally computationally intensive.[34] It has been shown that using DFT to study a large number of molecular geometries on the potential energy surface (PES), and then assessing the computed transition states using an ab initio method such as MP can be a reasonably accurate approach to calculate rate constants of self-initation reactions.[12,13] Salem and Rowland[40] reported spin−orbit coupling to be a common mechanism of intersystem crossing from singlet to triplet diradicals. In principle, crossover can occur, when a dense continuum of vibrational states is present in both singlet and triplet diradical and a few of these states are degenerate. Calculation of the spin−orbit coupling constant and using the constant in the Landau−Zener model[41]

provides a qualitative insight into whether the diradical species is inherently capable of transition from singlet to triplet state (high spin−orbit coupling constant) or requires external atoms to facilitate such a crossover (low spin−orbit coupling constant). The effect of solvent on the calculated energy barriers and rate constants of spontaneous initiation reactions can be assessed using solvent continuum models. Inclusion of these solvent models for toluene has been reported to show insignificant change in the calculated rate constants in comparison to the rate constants computed from gas-phase calculations.[21,42] In this study, solvent models have been neglected, and gas-phase calculations have been carried out.

This paper focuses on providing theoretical evidence as to whether spontaneous initiation in thermal polymerization of MMA occurs via diradical mechanism of self-initiation. It also investigates whether the stable diradical is singlet or triplet, and explores various mechanisms of monoradical generation. The singlet and triplet potential energy surfaces are constructed using B3LYP/6-31G*. Molecular geometries and transition states for formation of *cis*- and *trans*-DDCD, DMMH, and DAA are computed on the singlet surface. Validation of the calculated transition states on the singlet surface is carried out using MP2/6-31G*. Diradical intermediate formation on the triplet surface is investigated. The spin−orbit coupling mechanism is studied using MCSCF/6-31G*. Monoradical formation from the diradical and DAAs are explored, and the rates of monoradical formation via hydrogen abstraction and hydrogen transfer from the singlet and triplet diradicals are calculated.

This paper is organized as follows, section 2 discusses the computational methods used, section 3 gives results and discussion, and section 4 presents concluding remarks.

2. COMPUTATIONAL METHODS

All theoretical calculations are performed using GAMESS.[43] DFT[44] calculations on the singlet and triplet surfaces are performed using restricted open shell and unrestricted wave functions, respectively. B3LYP/6-31G*[45,46] is chosen as the level of theory to construct the potential energy surface profiles and estimate transition states due to its successful use in the study of free radical polymerization of alkenes[29,30] and self-initiation of styrene,[32] methyl acrylate,[12] ethyl acrylate, and *n*-butyl acrylate.[13] To our knowledge, this is the first DFT study for self-initiation of polymerization in MMA.

The molecular geometries of reactants, products, and transition states were optimized on the singlet and triplet surfaces. Hessian calculations are carried out to characterize reactants and transition states. Intrinsic reaction coordinate (IRC) calculations in the forward and reverse directions are conducted to determine minimum-energy pathways. Assessment of the transition states and energy barriers are performed with MP2/6-31G*. Energy barriers (relative to the energy of the reactant) are computed using the rigid rotor harmonic oscillator approximation.[47] Rate constants were computed by means of the transition state theory,[48] and the Wigner tunneling correction[49] was used. Reaction rate constants are calculated using

$$k(T) = \kappa(c^0)^{1-m}\frac{k_B T}{h} e^{\Delta S^{\ddagger}/R} e^{-\Delta H^{\ddagger}/RT} \quad (1)$$

where κ is the transmission coefficient, c^0 is the inverse of the reference volume assumed in calculating the translational partition function, $k(T)$ is the rate constant at temperature T, k_B is the Boltzmann constant, h is the Planck's constant, R is the universal gas constant, and $\Delta S^{\ddagger}$ and $\Delta H^{\ddagger}$ are the entropy and enthalpy differences between transition state and reactants, respectively. $\Delta H^{\ddagger}$ is given by

$$\Delta H^{\ddagger} = (E_0 + \mathrm{ZPVE} + \Delta\Delta H)_{\text{transition-reactants}} \quad (2)$$

where $\Delta\Delta H$ is the enthalpy correction factor, ZPVE is the zero point vibrational energy of the molecule, m is the molecularity of the reaction, and E_0 is the difference in electronic energy of transition state and reactants. The ZPVE, $\Delta\Delta H$, and $\Delta S^{\ddagger}$ are calculated at different temperatures using rigid rotor harmonic oscillator approximation.[47] The activation energy of each reaction, E_a, is calculated by

$$E_a = \Delta H^{\ddagger} + mRT \quad (3)$$

and the frequency factor, A, by

$$A = \kappa(c^0)^{1-m}\frac{k_B T}{h} e^{\Delta S^{\ddagger}/R} \quad (4)$$

Scaling factors to calculate the activation entropy, temperature correction, and zero point vibrational energy at different levels of theory are taken from the National Institute of Standards and Technology (NIST) Computational Chemistry Comparison and Benchmark Database.

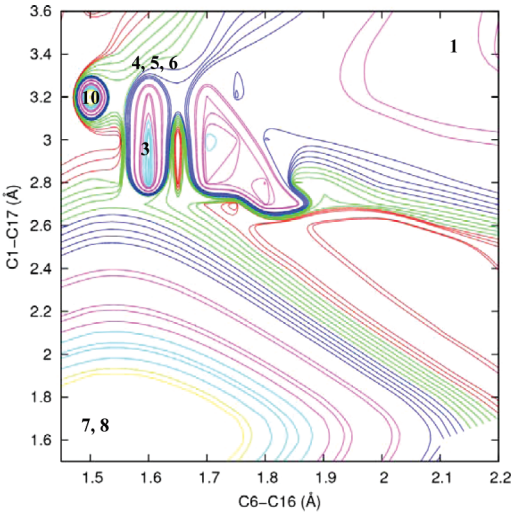

Figure 2. Singlet potential energy surface contour plot for the interaction of two MMA monomers as a function of two intermolecular carbon−carbon distances (Figure 3). Structure 1 is a pair of weakly interacting monomers (see Figure 3), structure 3 is the Diels−Alder adduct (DAA), structure 4 is the transition state for *trans*-DDCD formation (Figure 4), structure 5 is the transition state for *cis*-DDCD formation, structure 6 is the singlet diradical structure (Figure 5), structures 7 and 8 are *trans*- and *cis*-DDCD products (Figure 6), and structure 10 is the linear dimer DMMH (Figure 8). All contour lines represent energy relative to the reactants. Relative level of energy that each line represents: red > green > blue > pink > cyan > yellow. The energy difference between each two successive contour lines is 30 kJ mol^{-1}.

3. RESULTS AND DISCUSSION

The potential energy surface contour plot is constructed by constraining internuclear distances between 1.45 Å < r(C6−C16) < 2.2 Å and 1.6 Å < r(C1−C17) < 3.6 Å on the singlet surface as shown in Figure 2.

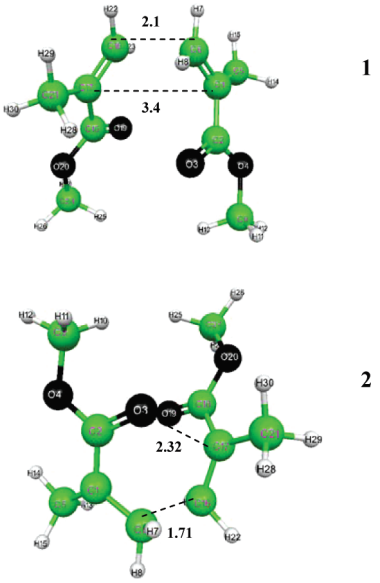

Figure 3. (**1**) Weakly interacting methyl methacrylate monomers; (**2**) transition state for DAA formation.

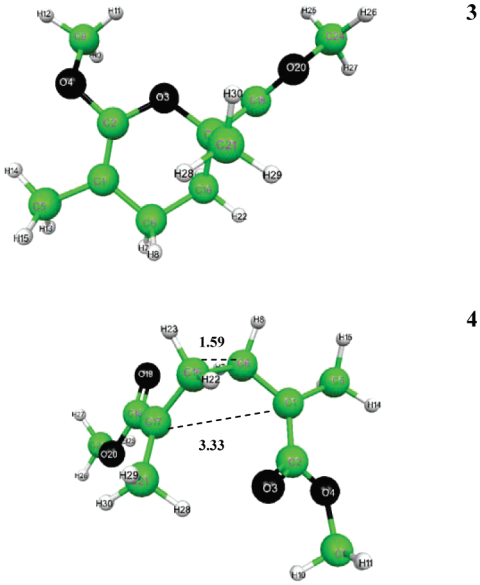

Figure 4. (**3**) DAA product via [4 + 2] cycloaddition reaction; (**4**) transition state for *trans*-DDCD formation.

Table 1. Bond length in Å, Activation Energy (E_a) in kJ mol^{-1}, Enthalpy (ΔH_{298}) in kJ mol^{-1}, and Rate Constant (k_{DAA}) in M^{-1} s^{-1} at 298 K Using Different Levels of Theory[a]

level of theory	r(C17−O3)	r(C6−C16)	E_a	ΔH_{298}	k_{DAA}
B3LYP/6-31G*	2.32	1.71	106.3	101.3	3.1×10^{-15}
MP2/6-31G*	2.28	1.66	82.7	77.6	1.4×10^{-10}

[a] The reported energies are zero point vibrational energy (ZPVE) corrected.

3.1. Singlet Surface: Diels−Alder Adduct (DAA) Formation. We found a thermal [4 + 2] cycloaddition reaction between C6═C1−C2═O3 of a MMA monomer and C16═C17 of another MMA monomer to form a Diels−Alder adduct (DAA) via a concerted pathway with a singlet transition state geometry, **2**. The transition state geometry for the formation of the DAA is r(C6−C16) = 1.71 Å, r(C17−O3) = 2.32 Å and ϕ(C1−C6−C16-C17) = 62.2° (Figure 3). IRC calculations were performed in the forward and the reverse directions to verify the transition state. We found a preference for the formation of a *meta*-like DAA. Table 1 depicts the energy barrier and rate constant for the formation of the DAA using different level of theory. The calculated barrier for the DAA formation (105 kJ mol^{-1}) is lower than those for the DAA formation in thermal polymerization of styrene (148 kJ mol^{-1})[32] and methyl acrylate (122 kJ mol^{-1}).[12] However, no DAA species have been found in spontaneous solution polymerization of MMA, even at low concentrations (≈10^{-3} mol L^{-1}).[14] The absence of DAA in solution indicates that at high temperatures the reverse Diels−Alder reaction is also occurring. In addition, the enthalpy of the DAA formation, computed from the difference between potential energies of the product and the reactants, is nearly zero, which shows that the reaction has little or no overall thermodynamic driving force. In view of these, we suggest that the DAA is not centrally involved in initiating thermal polymerization of MMA, although it is formed.

Validation studies of transition state geometry were performed using MP2/6-31G* level of theory. The transition state geometry is r(C6−C16) = 1.66 Å, r(C17−O3) = 2.28 Å, and ϕ(C1−C6−C16−C17) = 63.2°. As no in-laboratory experimentally obtained rate constant for the formation of DAA has been reported, a comparison is not possible.

3.2. Singlet Surface: Dimethyl 1,2-Dimethylcyclobutane-1,2-Dicarboxylate (DDCD) Formation. Thermal [2 + 2] cycloaddition between C1═C6 bond of a MMA monomer and C16═C17 of another MMA monomer was found to form a four-membered ring. We found a nonconcerted, single transition state and a flat potential energy surface with no energy minimum for the singlet diradical, for the formation of *cis*- and *trans*-isomers of DDCD using B3LYP/6-31G*, as shown in Figure 2. Figures 4−6 show the calculated transition state geometries and singlet diradical (•M•$_{2s}$) for *trans*-DDCD, **7**, and *cis*-DDCD, **8**, formation. The calculated distances, energy barriers, and rate constants using B3LYP/6-31G* and MP2/6-31G* are compared in Table 2. These computed activation energies showed good agreement with experimental predictions of 141 and 126 kJ mol^{-1}, for *cis*-DDCD and *trans*-DDCD formations, respectively.

Based on IRC calculations carried out using B3LYP/6-31G* in the forward and reverse directions from the transition states of *cis*-DDCD and *trans*-DDCD, a stereorandom one-step diradical mechanism is predicted for the formation of these dimers. This is in agreement with the pathway identified for spontaneous polymerization of pentafluorostyrene[50] and alkyl acrylates.[12,13] However, it was observed that the ring closure and DDCD formation was slower in MMA than in alkyl acrylates. To identify whether the methyl group on carbon atom C1 was retarding ring closure, the energy (relative to reactants) of the singlet diradical, **6**, as a function of dihedral angle ϕ(C5−C1−C6−C16) was studied by traversing at a step size of 30°, as shown in Figure 7. The favorable diradical conformation for rapid ring closure and formation of DDCD is most likely at ϕ(C5−C1−C6−C16) = 0. It can be seen from Figure 7 that a barrier of 7−8 kJ mol^{-1} has to be overcome for the singlet diradical in a gauche (ϕ = 60) conformation to reach ϕ = 0. We attribute the slower formation of DDCD in MMA than in methyl acrylates to this barrier. This barrier also caused an increase in the number of IRC

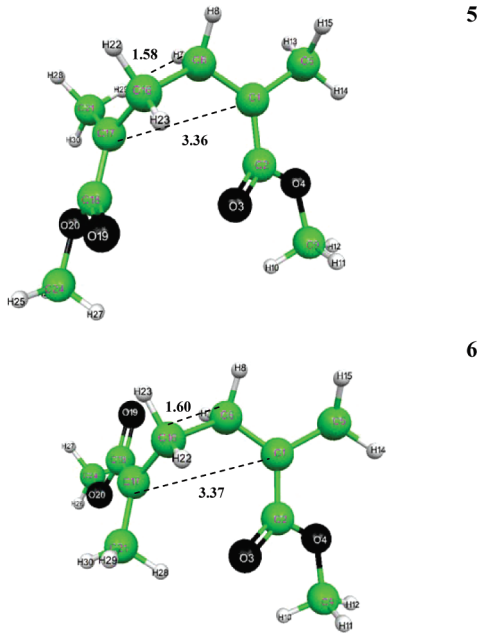

Figure 5. (**5**) Transition state for *cis*-DDCD formation; (**6**) singlet diradical species.

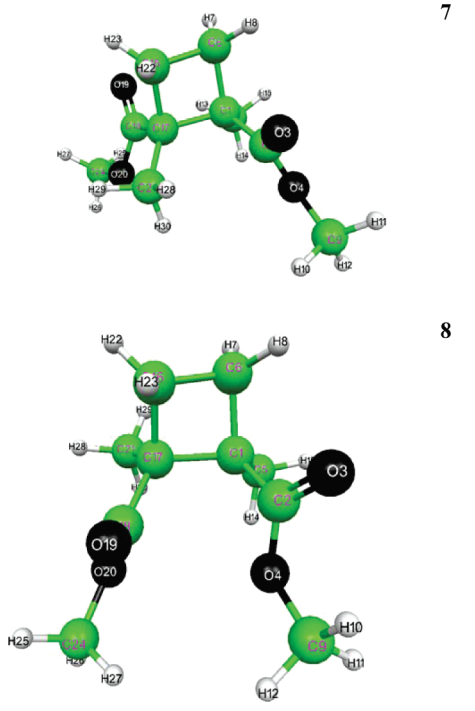

Figure 6. Products formed are **7** (*trans*-DDCD) and **8** (*cis*-DDCD).

steps, and perhaps this relates to an increase in the lifetime of the singlet diradical species. Thus, the reported low final concentrations of DDCD in solution[14,17] can be attributed to the possible preference of the singlet diradical to remain open rather than to undergo ring closure for DDCD formation.

3.3. Singlet Surface: Dimethyl 2-Methyl-5-Methylidene-Hexanedioate (DMMH) Formation. It was found that thermal [2 + 2] cycloaddition between C1═C6 and C16═C17 atoms can lead to the formation of DMMH via concerted pathway. The

Table 2. Bond Length in Å, Activation Energy (E_a) and Enthalpy (ΔH_{298}) in kJ mol^{-1}, and Rate Constant (k_{DDCD}) in M^{-1} s^{-1} at 298 K Using Different Levels of Theory[a]

level of theory	isomer	r(C17−C1)	r(C6−C16)	E_a	ΔH_{298}	k_{DDCD}
B3LYP/6-31G*	trans	3.33	1.59	188.2	183.3	1.8×10^{-29}
B3LYP/6-31G*	cis	3.36	1.58	226.3	221.4	3.8×10^{-36}
MP2/6-31G*	trans	3.20	1.55	123.2	118.3	1.9×10^{-17}
MP2/6-31G*	cis	3.18	1.54	146.2	141.3	1.8×10^{-21}

[a] The reported energies are zero point vibrational energy (ZPVE) corrected.

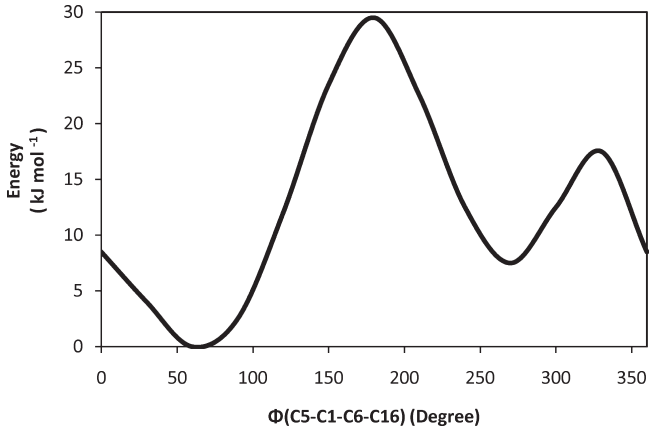

Figure 7. Rotation of the methyl group on carbon atom C1 of the singlet diradical. Energy of the diradical is relative to that of reactants vs dihedral angle, ϕ(C5−C1−C6−C16). See structure (**6**) in Figure 5. Positive rotation of the methyl group is into the page.

transition state geometry, **9**, was found to be r(C6−C17)=1.75 Å, r(C1−C16) = 3.05 Å, and ϕ(C1−C6−C17−C16) = −52.7°. The calculated DMMH geometry, **10**, was found to agree closely with the reported structures from laboratory experiments.[14,15] The formation of DMMH was observed to occur via intramolecular hydrogen (H16) transfer from the carbon atom (C22) on the first monomer to carbon atom (C1) on the second monomer (Figure 8). The energy barrier for the DMMH formation was calculated to be 116.8 kJ mol^{-1} using B3LYP/6-31G* and was calculated to be 96 kJ mol^{-1} using MP2/6-31G*. The calculated enthalpies and rate constants, given in Table 3, were found to be in good agreement with experimental values.[14]

The energy barrier of DMMH formation was found to be lower than that of DDCD. This indicates that DMMH formation will be kinetically preferred over DDCD formation, which agrees with previous experimental observations of higher concentration of DMMH in solution.[17] As the rapid DMMH formation can also retard the formation of diradical initiating species, it can be the cause for the slow rates of initiation reported in spontaneous polymerization of MMA in inert solvents such as benzene and toluene.[17] This indicates that the methyl group strongly influences spontaneous initiation in polymerization of MMA. Thus, we believe that the absence of linear dimer formation on the singlet potential energy surface of methyl, ethyl, and *n*-butyl acrylate, calculated using B3LYP/6-31G*,[12,13] and rapid rates of initiation in spontaneous polymerization of methyl acrylate and other acrylate monomers,[9,27,28] can be directly related to the lack of methyl group in acrylate monomers.

dx.doi.org/10.1021/jp107704h |*J. Phys. Chem. A* 2011, 115, 1125–1132

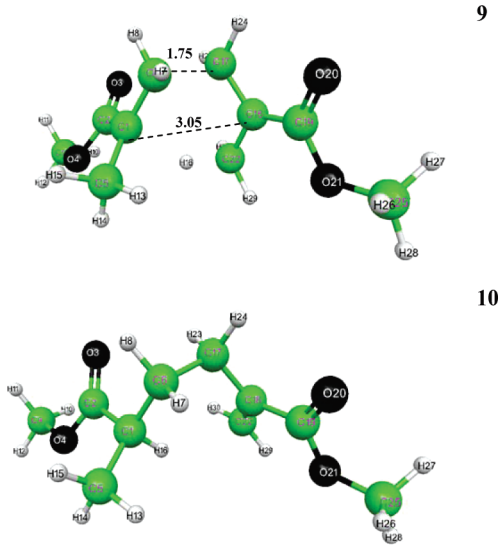

Figure 8. Formation of linear dimer DMMH via reaction between two MMA monomers: (**9**) transition state for DMMH formation; (**10**) DMMH product.

Table 3. Bond Length in Å, Activation Energy (E_a) and Enthalpy (ΔH_{298}) in kJ mol^{-1}, and Rate Constant (k_{DMMH}) in M^{-1} s^{-1} at 298 K Using Different Level of Theory[a]

level of theory	r(C18−C1)	r(C6−C17)	E_a	ΔH_{298}	Wigner[b]	k_{DMMH}
B3LYP/6-31G*	3.05	1.75	117.3	112.3	4.81	2.7×10^{-16}
MP2/6-31G*	2.88	1.65	97.2	92.3	4.81	3.3×10^{-12}

[a] The reported energies are zero point vibrational energy (ZPVE) corrected. [b] Wigner tunneling factor.

3.4. Triplet Surface. The triplet energy surface was explored using B3LYP/6-31G* by constraining coordinates between 1.5 Å < r(C6−C16) < 2.2 Å and 1.5 Å < r(C1−C17) < 3.4 Å, as shown in Figure 9. We found the presence of the triplet diradical intermediate, r(C6−C16) = 1.54 Å, r(C1−C17) = 3.25 Å, and ϕ(C1−C6−C16−C17) = 66.1° (Figure 9). This verifies previous reports[19,20] that the triplet diradical can be a key intermediate in initiating the polymerization. The energy difference between the singlet diradical transition state and the triplet diradical intermediate was found to be E_{S-T} = 80 kJ mol^{-1}, which is approximately 2 kJ mol^{-1} higher than that reported for methyl acrylate.[12] The minimum energy crossing point from the singlet to triplet was computed using B3LYP/6-31G*. This geometry was optimized using MCSCF/6-31G* and then the molecular orbitals from MCSCF were used to calculate the spin−orbit coupling constant.

The spin−orbit coupling constant was calculated by including the full Breit-Pauli operator.[51] The calculated spin−orbit coupling constant was 2.5 cm^{-1}. Using Landau−Zener model, we can suggest that such a low value of the spin−orbit coupling constant corresponds to lower transition probability from singlet to triplet diradical. Therefore, interaction with additional heavy atoms and inert gases[22,23] becomes important for crossover in MMA. This agrees with the conclusions drawn after observing higher rates of initiation in polymerization of MMA in halogenated solvents bubbled with nitrogen or argon.[19,20]

3.5. Monoradical Generation. Previous studies[19] based on experimental measurements fitted to macroscopic mechanisitic

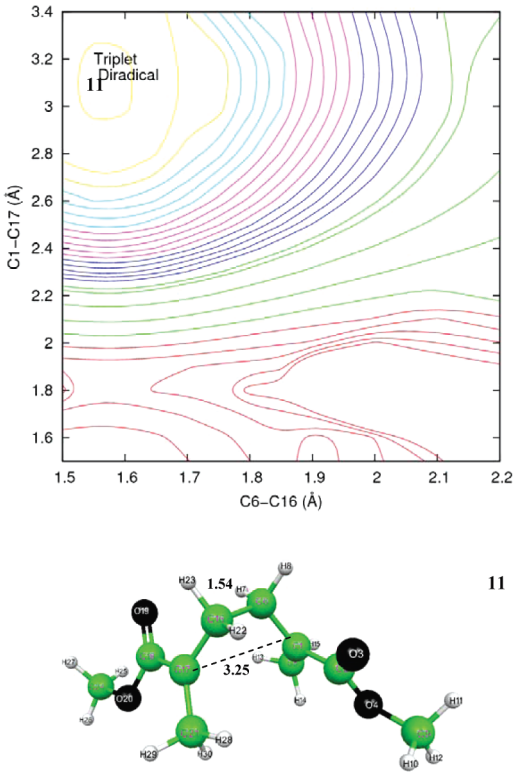

Figure 9. Triplet potential energy surface of methyl methacrylate dimerization; (**11**) triplet diradical intermediate. All contour lines represent energy relative to the reactants. Relative level of energy that each line represents: red > green > blue > pink > cyan > yellow. The energy difference between each two successive contour lines is 30 kJ mol^{-1}.

models have postulated that the triplet diradical initiates polymerization of MMA. Calculations using B3LYP/6-31G* were carried out to verify the occurrence of this mechanism and also investigate other mechanisms of monoradical generation. Hydrogen transfer from DAA to a third monomer, molecular assisted homolysis (MAH) mechanism, was studied by constraining intermolecular distances between 1.19 Å < r(C31−H29) < 1.59 Å and 1.19 Å < r(H29−C21) < 1.59 Å. It was observed that DAA was incapable of donating a hydrogen to the third monomer, which was in agreement with previous reports on MMA and alkyl acrylates.[1,12,13,15]

Based on our previous studies of self-initiation in methyl acrylate, we chose to study the singlet and triplet diradicals, donating (hydrogen transfer) and accepting (hydrogen abstraction) a hydrogen from a third MMA monomer. Reaction coordinates were constrained between 1.19 Å < r(C1−H31) < 1.59 Å and 1.19 Å < r(H31−C32) < 1.59 Å to study hydrogen transfer from a third monomer to the diradical, and between 1.19 Å < r(C6−H7) < 1.59 Å and 1.19 Å < r(H7−C31) < 1.59 Å to investigate hydrogen abstraction from a third monomer to the diradical.

Stable transition state geometries for hydrogen abstraction by the singlet and triplet diradicals from a third monomer and hydrogen transfer from the triplet diradical to a third monomer were calculated. No transition state was identified for hydrogen transfer from singlet diradical to a third monomer. This provides further support that molecular assisted homolysis may be an unfavorable mechanism in MMA. It was found that the energy

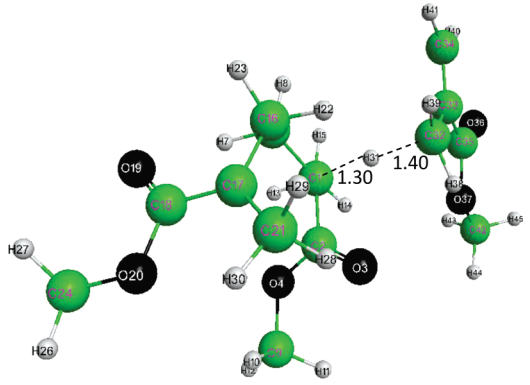

Figure 10. Hydrogen abstraction by a singlet diradical from a third monomer; (**13**) transition state geometry. Bond lengths shown are in Å.

barrier for hydrogen abstraction by the singlet and triplet diradicals from a third monomer was signifcantly lower than hydrogen transfer from the triplet diradical to a third monomer. This is dissimilar to the mechanism of monoradical generation reported in methyl acrylate.[12] This points to the strong involvement of singlet and triplet diradicals as a key intermediates for the generation of monoradical species in spontaneous thermal polymerization of MMA. It is interesting to note that intramolecular hydrogen transfer, from the methyl group to the carbon atom with an unpaired electron, in the singlet diradical causes DMMH formation (dead polymer chain), and intermolecular hydrogen abstraction by the singlet diradical from a third monomer generates monoradical species for initiating the polymerization. On the basis of the calculated rate constants, these reactions may be competing with each other and may have equal probability of occurrence. Thus, we attribute the reported[1] lower conversion and higher molecular weight polymer formation to these reactions. This points to the strong influence of the methyl group on the diradical self-initiation mechanism in MMA. The calculated transition state geometries are shown in Figures 10−12. The energy barriers and rate constants for the hydrogen transfer and hydrogen abstraction reactions are given in Table 4.

3.6. Comparison of Self-Initiation in Methyl Methacrylate and Methyl Acrylate. We have shown through quantum chemical calculations that monomer self-initiation occurs in spontaneous high-temperature polymerization of MA[12] and MMA (this study). The diradical mechanism of self-initiation was determined to be dominant in self-initiated polymerization of both the monomers. The Diels−Alder adduct (DAA) formation was identified to occur via a concerted pathway and the formation of singlet diradical was found to be via nonconcerted pathway for MA and MMA. The activation energy calculated using DFT/6-31G* for the formation of DAA in MA (123 kJ mol^{-1}) was higher in comparison to that of MMA (106 kJ mol^{-1}) and for cyclobutane dimer formation was comparable between MA (191 kJ mol^{-1}) and MMA (188.2 kJ mol^{-1}). Formation of DMMH was found in MMA and not in MA. The formation of triplet diradical via intersystem crossing of the singlet diradical was predicted to be through the mechanism of spin−orbit coupling. The spin−orbit coupling constant of MA and MMA were found to be 1.94 and 2.5 cm^{-1}, respectively. Monoradical generation was identified to be not possible from Diels−Alder's adduct in both cases. While the triplet diradical was found to be involved in monoradical generation in MA, both singlet and triplet diradicals were identified as key intermediates

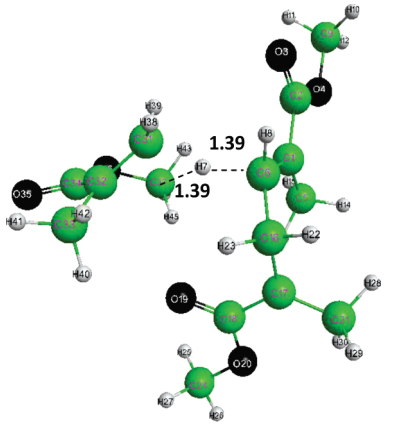

Figure 11. Hydrogen transfer from a triplet diradical to a third monomer; (**14**) transition state geometry. Bond lengths shown are in Å.

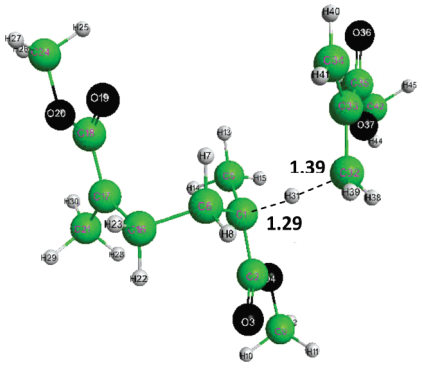

Figure 12. Hydrogen abstraction by a triplet diradical from a third monomer; (**15**) transition state geometry. Bond lengths shown are in Å.

Table 4. Activation Energy (E_a) and Enthalpy (ΔH_{298}) in kJ mol^{-1}, and Rate Constant (M^{-1} s^{-1}) for Monoradical Formation[a]

reaction	E_a	ΔH_{298}	Wigner[b]	k
i	98.1	93.2	4.81	3.8×10^{-10}
ii	175.5	170.1	4.81	6.4×10^{-23}
iii	102.1	97.2	4.81	7.7×10^{-11}

[a] Via (i) hydrogen abstraction by $\bullet M\bullet_{2s}$ from MMA, (ii) hydrogen transfer from $\bullet M\bullet_{2t}$ to MMA and (iii) hydrogen abstraction by $\bullet M\bullet_{2t}$ from MMA. The reported energies are zero point vibrational energy (ZPVE) corrected and at temperature of 298 K. [b] Wigner tunneling factor.

in monoradical formation in MMA. Hydrogen abstraction by the singlet and triplet diradicals from a third monomer were calculated to be the preferred mechanisms in MMA. Hydrogen transfer from the triplet diradical to a third monomer was found to be the lower energy pathway in MA. It is to be noted that ethyl acrylate (EA) and *n*-butyl acrylate (*n*BA)[13] showed similar behavior to MA.[12] Our comparisons between MA and MMA are therefore likely to apply also to comparison of EA−*n*BA monomers and MMA.

4. CONCLUSIONS

The formation of DAA, DMMH, and DDCD on the singlet surface was identified using B3LYP/6-31G* calculations. DMMH

dx.doi.org/10.1021/jp107704h |*J. Phys. Chem. A* 2011, 115, 1125–1132

and DAA formation was found to occur via a concerted pathway, and DDCD formation via a nonconcerted pathway. The energy barriers for DMMH and DDCD formation were found to be higher than that of DAA and comparable to energy barrier values obtained experimentally.[1,15] We found the presence of a low energy diradical intermediate on the triplet surface, which substantiates the postulate of Pryor and Laswell.[8] The mechanism of spin−orbit coupling for crossover from singlet to triplet was proposed, and spin−orbit coupling constant was calculated to be 2.5 cm^{-1} using MCSCF/6-31G*. It was found that monoradical formation is most likely to occur via hydrogen abstraction by both singlet and triplet diradicals from a third MMA monomer. This study validated previous experimental studies[1,14,15] and provided new evidence for the diradical mechanism of self-initiation and for the abstraction mechanism of monoradical generation in spontaneous thermal polymerization of methyl methacrylate.

AUTHOR INFORMATION

Corresponding Author
*E-mail: soroushm@drexel.edu.

ACKNOWLEDGMENT

S.S. and M.S. acknowledge the National Science Foundation (NSF) through Grant CBET-0932882. Acknowledgment is also made to the Donors of the American Chemical Society Petroleum Research Fund for partial support of this research. A.M.R. acknowledges the NSF through the Grant CBET-0932786, and M.W.L. acknowledges the U.S. Air Force Office of Scientific Research for support under Grant FA9550-10-1-0248. Computational support was provided by the High-Performance Computing Modernization Office of the U.S. Department of Defense.

REFERENCES

(1) Stickler, M.; Meyerhoff, G. *Makromol. Chem.* **1978,** *179*, 2729.
(2) Mayo, F. R. *J. Am. Chem. Soc.* **1953,** *75*, 6133.
(3) Flory, P. J. *J. Am. Chem. Soc.* **1937,** *59*, 241.
(4) Walling, C.; Briggs, E. R. *J. Am. Chem. Soc.* **1946,** *68*, 1141.
(5) Hiatt, R. R.; Bartlett, P. D. *J. Am. Chem. Soc.* **1959,** *81*, 1149.
(6) Mayo, F. R. *J. Am. Chem. Soc.* **1968,** *90*, 1289.
(7) Buzanowski, W. C.; Graham, J. D.; Priddy, D. B.; Shero, E. *Polymer* **1992,** *33*, 3055.
(8) Pryor, W. A.; Lasswell, L. D. In *Advances In Free Radical Chemistry;* Williams, G. H., Ed. Academic Press, New York, NY, 1975, Vol. V, pp 27−99.
(9) Grady, M. C.; Quan, C.; Soroush, M. U.S. Patent Application Number 60/484,393, filed on July 2, 2003.
(10) Breitenbach, J. W.; Raff, R. *Chem. Ber* **1936,** *69*, 1107.
(11) Lehrle, R. S.; Shortland, A. *Eur. Polym. J.* **1988,** *24*, 425.
(12) Srinivasan, S.; Lee, M. W.; Grady, M. C.; Soroush, M.; Rappe, A. M. *J. Phys. Chem. A* **2009,** *113*, 10787.
(13) Srinivasan, S.; Lee, M. W.; Grady, M. C.; Soroush, M.; Rappe, A. M. *J. Phys. Chem. A* **2010,** *114*, 7975.
(14) Stickler, M.; Meyerhoff, G. *Makromol. Chem.* **1980,** *181*, 131.
(15) Brand, E.; Stickler, M.; Meyerhoff, G. D. *Makromol. Chem.* **1980,** *181*, 913.
(16) Lingnau, J.; Stickler, M.; Meyerhoff, G. *Eur. Polym. J.* **1980,** *16*, 785.
(17) Stickler, M.; Meyerhoff, G. *Polymer* **1981,** *22*, 928.
(18) Lingnau, J.; Meyerhoff, G. *Polymer* **1983,** *24*, 1473.
(19) Lingnau, J.; Meyerhoff, G. *Makromol. Chem.* **1984,** *185*, 587.
(20) Lingnau, J.; Meyerhoff, G. *Macromolecules* **1984,** *17*, 941.
(21) Gilbert, R. G. *Pure Appl. Chem.* **1996,** *7*, 1491.
(22) Robinson, G. W. *J. Chem. Phys.* **1967,** *47*, 1967.
(23) Kropp, P. J. *J. Am. Chem. Soc.* **1969,** *91*, 5783.
(24) Woodward, R. B.; Hoffmann, R. *J. Am. Chem. Soc.* **1965,** *87*, 395.
(25) Quan, C. *Ph.D. Thesis*, Drexel University, Philadelphia, PA, 2002.
(26) Quan, C.; Soroush, M.; Grady, M. C.; Hansen, J. E.; Simonsick, W. J. *Macromolecules* **2005,** *38*, 7619.
(27) Rantow, F. S.; Soroush, M; Grady, M. C.; Kalfas, G. A. *Polymer* **2006,** *47*, 1423.
(28) Srinivasan, S.; Kalfas, G.; Petkovska, V. I.; Bruni, C.; Grady, M. C.; Soroush, M. J. *Appl. Polym. Sci.* **2010,** *118* (4), 1898.
(29) Wong, M. W.; Radom, L. *J. Phys. Chem.* **1995,** *99*, 8582.
(30) Van Cauter, K.; Van Speybroeck, V.; Vansteenkiste, P.; Reyniers, M. F.; Waroquier, M. *ChemPhysChem* **2006,** *7*, 131.
(31) Gunaydin, H.; Salman, S.; Tuzun, N. S.; Avci, D.; Aviyente, V. *Int. J. Quant. Chem.* **2005,** *103*, 176.
(32) Khuong, K. S.; H. Jones, W. H.; Pryor, W. A.; Houk, K. N. *J. Am. Chem. Soc.* **2005,** *127*, 1265.
(33) Cohen, A. J.; Mori-Sanchez, P.; Yang, W. *Science* **2008,** *321*, 792.
(34) Coote, M. L. *Encyclopedia of Polymer Science and Technology*; Wiley Interscience: New Jersey, 2006; Vol. 1.
(35) Pople, J. A.; Head-Gordon, M.; Fox, D. J.; Raghavachari, K.; Curtiss, J. *J. Chem. Phys.* **1989,** *90*, 5622.
(36) Curtiss, L. A.; Raghavachari, K.; Trucks, G. W.; Pople, J. A. *J. Chem. Phys.* **1991,** *94*, 7221.
(37) Curtiss, L. A.; Raghavachari, K.; Redfern, C.; Rassolov, V.; Pople, J. A. *J. Chem. Phys.* **1998,** *109*, 7764.
(38) Curtiss, L. A.; Raghavachari, K. *Theor. Chem. Acc.* **2002,** *108*, 61.
(39) Curtiss, L. A.; Redfern, P. C.; Raghavachari, K. *J. Chem. Phys.* **2007,** *126*, 084108.
(40) Salem, L.; Rowland, C. *Angew. Chem., Int. Ed.* **1972,** *11*, 92.
(41) Landau, L. *Phys. Sov. U.* **1932,** *2*, 46. Zener, C. *Proc. R. Soc. London, Ser. A* **1932,** *137*, 692.
(42) Yu, X.; Pfaendtner, J.; Broadbelt, L. J. *J. Phys. Chem. A* **2008,** *112*, 6772.
(43) Schmidt, M. W.; Baldridge, K. K.; Boatz, J. A.; Elbert, S. T.; Gordon, M. S.; Jensen, J. H.; Koseki, S.; Matsunaga, N.; Nguyen, K. A.; Su, S. J.; Windus, T. L.; Dupuis, M.; Montgomery, J. A. *J. Comput. Chem.* **1993,** *14*, 1347–1363 available at http://www.msg.ameslab.gov/GAMESS/GAMESS.html.
(44) Hohenberg, P.; Kohn, W. *Phys. Rev.* **1964,** *136*, 864.
(45) Becke, A. D. *Phys. Rev. A* **1988,** *38*, 3098.
(46) Lee, C.; Yang, W.; Parr, R. G. *Phys. Rev. B* **1988,** *37*, 785.
(47) Irikura, K. K. *THERMO.PL*; National Institute of Standards and Technology: Gaithersburg, MD, 2002.
(48) Eyring, E. *J. Chem. Phys.* **1935,** *3*, 107.
(49) Wigner, E. P. *Z. Phys. Chem.* **1932,** *19*, 203.
(50) Dervan, P. B.; Santilli, D. S. *J. Am. Chem. Soc.* **1980,** *102*, 3863.
(51) Fedorov, D. G.; Koseki, S.; Schmidt, M. W.; Gordon, M. S. *Int. Rev. Phys. Chem.* **2003,** *22*, 551.